Continuum Models for Systems in a Selfstress State

K. Kébiche, Nadjib M. Kazi-Aoual, René Motro

Continuum Models for Systems in a Selfstress State

K. Kebiche[1], M. N. Kazi Aoual[2], and R. Motro[2]

[1]Laboratoire d'Architecture Méditerranéenne, University of Setif, Algeria
[2]Laboratoire de Mécanique et Génie Civil, place E. Bataillon Université Montpellier II, France

ABSTRACT: We present a procedure to determine continuum equivalent properties of systems in selfstress state; this procedure is based on the energetic equivalence between the discrete model and the continuum model. This equivalence expresses the identity between strain energy and the selfstress energy developed in both models. Research of equivalent continuum media is made in the vicinity of the non-deformed configuration. The application of this procedure to tensegrity systems is validated on three types of modules, the simplex, the regular quadruplex (vertically **homogenized**) and the half-cuboctahedron quadruplex (horizontally **homogenized**). The equivalent rigidities and the coupling terms obtained on these modules are presented and compared to those obtained by a direct method (finite element method). Particular interest is paid to the influence of selfstress on the equivalent rigidities and the coupling terms of the continuum model.

Key Words: Tensegrity, homogenization, selfstress, equivalent rigidity, continuum model.

1. INTRODUCTION

The main issue in the study of repetitive elongated strut, or strut-and-cable structures consists in trying to optimize computation methods, making them as simple and as fast as possible. This is particularly true when the main characteristic of these structures is their geometric complexity. Thus, we were interested in finding an equivalent continuous media with globally the same properties as the discrete structure but easier to study; getting this equivalent continuous media would help to simplify the mechanical studies. The concept of homogenization, relatively new in this kind of structures, will enable us to translate the mechanical behaviour on a macroscopic scale of a beam for example from the microscopic behaviour of a basic cell. So the periodic character of the structure could usefully be taken into account, since we would only need to study one single cell as compared to other methods for which the difficulty increases with the number of modules.

In this paper, we study a class of innovative systems in the field of spatial structures: systems in a selfstress state. There exist reticulate strut-and-cable systems, where the rigidity and the stability are conditioned by the existence of a selfstress state. In a modular structure of this family, each module can have a different self-stress level, and in horizontal quadruplex assemblies with more than two modules, it has been established that the number of selfstress states is higher than that of the modules. Interested reader can examine the literature concerning tensegrity systems for classical issues, our introduction is dedicated to new approaches of homogenization.

Concerning this specific topic, homogenization techniques based on the use of asymptotic development in double scale can be mentioned: these techniques have been developed by Verna & Caillerie [1] and [2] who studied the behaviour of platelike lattices in static configuration (N, X and W beams); in their study, the displacements and the tensions in the struts are written in the form of an asymptotic development compared to a small parameter ε. The macroscopic behaviour of the beam is obtained by exploiting different orders of the parameter ε in equilibrium equations. Tollenaere [3] uses the same procedure in the case of free vibrations,

first of all on a one-dimensional system composed of concentrated masses and springs, then in the case of vibrations of the platelike lattices with pin jointed nodes. Ohayon [4] uses the method of asymptotic developments in double scale to study the harmonic vibrations of a heterogeneous ring with a repetitive configuration. The advantage of this approach is that the equivalent continuum model still keeps all the degrees of freedom of the discrete model, which enables a back path to local behaviour. On the other hand this method is characterised by a very heavy mathematical formalism, which restricts its application to only very simple geometries. Another technique is simultaneously developed, it is based on a concept of energy equivalence.

Noor et al. [5] and [6] use this method to study three-dimensional beamlike lattices with pin jointed nodes and rigid nodes. To define the fields of displacement they use a Taylor series development along the longitudinal axis of the beam where they make the strain and the strain gradient appear. Noor & Nemeth [7] take an hypothesis of micro-polar continuous media into account, and they define fields of displacement and rotation along the three spatial directions. Compared with finite element computation, they obtain results of less than 2% error on the displacements and the rotations.

Dow et al. [8] suggest a more general approach than that of Noor by writing a matricial formulation; they use a polynomial approximation of the field displacement (order of 3). The 60 coefficients that appear, are identified by using linear elasticity equations (strain-displacement relations). According to the geometric complexity of the basic cell, a reduction of the number of coefficients is suggested, either by determining the rank of a transformation matrix, or by introducing kinematic hypotheses on the continuum model (for example the Love-Kirchhoff hypotheses).

McCallen and Romstad [9] use the concept of energy equivalence in the hypothesis of geometrical non-linearities on a simple flat structure (X cell). They use the notion of generalized stress in the cross-section so as to write the strain energy in the lattice model. This approach is also used in other particular applications: in dynamic approaches Abrate and Sun [10] model a beamlike lattice taking into account viscous damping, Banks et al.[11], Juang et al.[12] use the continuum model for the dynamic identification of a lattice. Yang et al.[13] use this approach for the dynamic testing of spatial structures and Bazant [14] studies the problem of checking the buckling situations for rigid node lattices with the continuum model.

In our work, aiming to **homogenize** systems in tensegrity state, we use the concept of energy equivalence as developed by Dow et al. [8], but taking into account the selfstress. That is to say, the total strain energy stored in the discrete system will be the sum of two terms, one caused by the elastic rigidity of the elements and the other by the initial selfstress. It must be recalled that we may as well apply this procedure for tensegrity systems assuming that the assemblies of the different modules be linear. In other terms, they constitute repetitive beams. Once the assemblies of modules become two-dimensional, such as the grids, the procedure is invalid.

The research of equivalent continuum media is made in the vicinity of the initial, non-deformed configuration. But it is possible to apply this procedure in the geometric non-linear behaviour situations. And this is our objective in the future (this work is on progress), to use these equivalent rigidities in the beam finite element rigidity matrix to try to approach the geometric non-linear behaviour of beams with several modules. In this stage, we proceed step by step, and for each load step we recalculate the equivalent rigidities associated with the new configurations.

2. THE SELFSTRESS CONTINUUM MODEL

It could be useful to remember at this point that the equivalent continuum model we are looking for will also be selfstressed. Characterized on one hand by the six terms of rigidity (longitudinal rigidity $\overline{EA}$, the flexural rigidities $\overline{EI}_y$ and $\overline{EI}_z$, shearing rigidities $\overline{GA}_y$ and $\overline{GA}_z$ and torsional rigidity $\overline{GJ}$) and on the other hand by the coupling terms c_{ij}. These coupling terms are null in the case of a cell with symmetrical geometry. The equilibrium of a continuum beam for which transversal shearing is taken into account can be translated by the following equation:

$$\begin{bmatrix} N \\ M_y \\ M_z \\ V_y \\ V_z \\ C_t \end{bmatrix} = \begin{bmatrix} \overline{EA} & c_{12} & c_{13} & c_{14} & c_{15} & c_{16} \\ c_{12} & \overline{EI}_y & c_{23} & c_{24} & c_{25} & c_{26} \\ c_{13} & c_{23} & \overline{EI}_z & c_{34} & c_{35} & c_{36} \\ c_{14} & c_{24} & c_{34} & \overline{GA}_z & c_{45} & c_{46} \\ c_{15} & c_{25} & c_{35} & c_{45} & \overline{GA}_y & c_{56} \\ c_{16} & c_{26} & c_{36} & c_{46} & c_{56} & \overline{GJ} \end{bmatrix} \begin{bmatrix} \varepsilon_x^0 \\ k_y^0 \\ k_z^0 \\ \gamma_{xy}^0 \\ \gamma_{xz}^0 \\ k_t^0 \end{bmatrix} \quad (1)$$

$$\text{So that } \overline{EA} = EA^0 + EA^q \text{ et } \overline{EI}_y = EI_y^0 + EI_y^q \text{ .....etc} \quad (2)$$

$$c_{ij} = c_{ij}^0 + c_{ij}^q$$

Where the index « 0 » indicates elastic rigidity of the elements, and the index « q » indicates rigidity due to initial selfstress.

N is the axial force, M_y and M_z the bending moments according to the axes y and z, V_y and V_z the shear forces according to y and z and C_t the torsion couple around the neutral axis. ε_x is the longitudinal strain of the beam, k_y^0 and k_z^0 the bending curvatures associated respectively to M_y and M_z, γ_{xy}^0 and γ_{xz}^0 the transverse shear strain, k_t^0 is the torsion strain.

The strain energy U_c of a continuum beam without coupling terms is expressed as follows:

$$\begin{aligned} U_c = \frac{1}{2}\int_0^l (&\overline{EA}\left(\varepsilon_x^0\right)^2 + \overline{EI}_y\left(k_y^0\right)^2 + \overline{EI}_z\left(k_z^0\right)^2 \\ &+\overline{k}_y\overline{GA}_y\left(\gamma_{xy}^0\right)^2 + \overline{k}_z\overline{GA}_z\left(\gamma_{xz}^0\right)^2 \\ &+\overline{GJ}\left(k_t^0\right)^2)\ dx \end{aligned} \tag{3}$$

Where k_y and k_z are the correction shear factors.

3. THE DISCRETE SELFSTRESS MODEL

The expression of the total strain energy of a pin jointed structure in a selfstress state is:

$$\begin{aligned} U_d &= \frac{1}{2}\{u\}_i^T\left[\left[K_{EA}\right]+\left[K_G\right]\right]\{u\}_i \\ &= \frac{1}{2}\{u\}_i^T\left[K_d^{Total}\right]\{u\}_i \end{aligned} \tag{4}$$

Where $[K_{EA}]$ is the matrix of linear stiffness, $[K_G]$ is the matrix of the initial stresses given in the case of an element (k) expressed in the local reference axis:

$$\left[K_G^{(k)}\right] = q^{(k)}.\begin{bmatrix} 1 & 0 & 0 & -1 & 0 & 0 \\ 0 & 1 & 0 & 0 & -1 & 0 \\ 0 & 0 & 1 & 0 & 0 & -1 \\ -1 & 0 & 0 & 1 & 0 & 0 \\ 0 & -1 & 0 & 0 & 1 & 0 \\ 0 & 0 & -1 & 0 & 0 & 1 \end{bmatrix} \tag{5}$$

where $q^{(k)} = \dfrac{T^{(k)}}{L^{(k)}}$ is the coefficient of force density, and :

$$\left[K_d^{Total}\right] = \left[K_{EA}\right]+\left[K_G\right] \tag{6}$$

The variables in the expression (4) are the nodes displacements; they must be transformed and expressed in function of the variables appearing in the continuum model, (1) and (3). Then a simple comparison between the two expressions will enable the deduction of the equivalent rigidity. The procedure for this transformation will now be summarized in the following paragraphs.

3.1. First transformation $[T_1]$

This transformation consists in defining a field of displacement (u, v and w), in the form of a polynomial expansion of 3-order, with respect to the local cell reference. The choice of such an order of expansion is sufficient to model the tensegrity modules, the second order of polynomial is sufficient for modelling the three modules of tensegrity firstly studied in this paper. By contrast, the third order is necessary for modelling other modules of tensegrity such as the expanded octahedron (a module with 6 struts and 24 cables).

$$u(x,y,z)=a_1+a_2x+a_3y+a_4z+a_5x^2+a_6xy+.....+a_{20}z^3$$

$$v(x,y,z)=b_1+b_2x+b_3y+b_4z+b_5x^2+b_6xy+.....+b_{20}z^3 \tag{7}$$

$$w(x,y,z)=c_1+c_2x+c_3y+c_4z+c_5x^2+c_6xy+.....+c_{20}z^3$$

A total of 60 coefficients appear in this field of displacement (ai, bi and ci with i = 1,20), these coefficients are calculated with respect to strains and strains gradients using the equations of elasticity. Once these coefficients have been determined, the polynomial expansion is then applied to all degrees of freedom of the base cell (3xn); n is number of nodes.

$$\begin{Bmatrix} u_1 \\ v_1 \\ w_1 \\ u_2 \\ v_2 \\ \\ \\ w_n \end{Bmatrix}_i = \begin{bmatrix} 1 & 0 & 0 & x_1 & 0 & . & . & -\frac{1}{6}z_1^3 \\ 0 & 1 & 0 & 0 & y_1 & . & . & 0 \\ 0 & 0 & 1 & 0 & 0 & . & . & \frac{1}{2}x_1z_1^2 \\ 1 & 0 & 0 & x_2 & 0 & . & . & -\frac{1}{6}z_1^3 \\ 0 & 1 & 0 & 0 & y_2 & . & . & 0 \\ . & . & . & . & . & . & . & . \\ . & . & . & . & . & . & . & . \\ 0 & 0 & 1 & 0 & 0 & . & . & \frac{1}{2}x_nz_n^2 \end{bmatrix} . \begin{Bmatrix} u^0 \\ v^0 \\ w^0 \\ \varepsilon_x^0 \\ \varepsilon_y^0 \\ \\ \\ \varepsilon_{z,xz}^0 \end{Bmatrix} \tag{8}$$

Or in an abbreviated form: $\{u\}_i = [T_1]\{u\}_\varepsilon$,

where $\{u\}_i$ is the displacements vector defined by the finite elements model of dimension n, $\{u\}_\varepsilon$ the vector of the strains and of their derivatives of dimension 60, and $[T_1]$ the first matrix of rectangular transformation of dimension (3nx60). This matrix obviously depends only on the geometry of the cell. In reference [8],

Dow et al. clearly explain the calculation procedure of the (3nx60) coefficients.

From this transformation, the strain energy of the base cell can be written in function of the vector $\{u\}_\varepsilon$:

$$\begin{aligned} U_d &= \frac{1}{2}\{u\}_i^T\left[[K_{EA}]+[K_G]\right]\{u\}_i \\ &= \frac{1}{2}\{u\}_\varepsilon^T[T_1]^T\left[K_d^T\right][T_1]\{u\}_\varepsilon \end{aligned} \quad (9)$$

3.2. Second transformation [T_2]

The following transformation consists in reducing the number of variables of the vector $\{\mathbf{u}\}_\varepsilon$. As long as the freedom degrees number of the base cell is less than 60, which is in fact often the case, linearly dependent variables can be found among these components. These can then be eliminated by calculating the rank of the matrix of the first transformation matrix [T_1].

The transformation matrix [T_2] enables to link of the strain vector $\{u\}_\varepsilon$ of dimension 60 with the new strain vector obtained after transformation matrix [T_2]:

$$\{u\}_\varepsilon = [T_2]\ \{\mu\}_\varepsilon \quad (10)$$

$\{\mu\}_\varepsilon$ is the new strain vector obtained after transformation [T_2]. It must be recalled that the first six components of $\{\mathbf{u}\}_\varepsilon$ must be preserved in $\{\mu\}_\varepsilon$ for decomposition in the third transformation. By substituting the vector $\{\mu\}_\varepsilon$ in the expression of the strain energy given by (9):

$$U_d = \frac{1}{2}\{\mu\}_\varepsilon^T[T_2]^T[T_1]^T\left[K_d^T\right][T_1][T_2]^T\ \{\mu\}_\varepsilon \quad (11)$$

is obtained.

3.3. Third transformation [T_3]

The following transformation consists in decomposing the strain vector $\{\mu\}_\varepsilon$ obtained after the previous transformation in two parts; the first noted $\{\alpha\}_\varepsilon$, includes the six strain components appearing in the strain energy expression (3), the second part of the vector $\{\mu\}_\varepsilon$ is written as $\{\beta\}_\varepsilon$; this vector assembles the remaining variables.

The transformation matrix [T_3] operates this decomposition with the following formula:

$$\{\mu\}_\varepsilon = [T_3].\begin{Bmatrix}\alpha\\ \beta\end{Bmatrix}_\varepsilon \quad (12)$$

$$U_d = \frac{1}{2}\begin{Bmatrix}\alpha\\ \beta\end{Bmatrix}_\varepsilon^T[T_3]^T[T_2]^T[T_1]^T\left[K_d^T\right][T_1][T_2][T_3]\begin{Bmatrix}\alpha\\ \beta\end{Bmatrix}_\varepsilon \quad (13)$$

That can be put as follows:

$$U_d = \frac{1}{2}\begin{Bmatrix}\alpha\\ \beta\end{Bmatrix}_\varepsilon^T[D]\begin{Bmatrix}\alpha\\ \beta\end{Bmatrix}_\varepsilon \quad (14)$$

with:

$$[D] = [T_3]^T[T_2]^T[T_1]^T\left[K_d^T\right][T_1][T_2][T_3] \quad (15)$$

3.4. Fourth transformation [T_4]

This transformation consists in expressing the vector $\{\beta\}_\varepsilon$ in function of the vector $\{\alpha\}_\varepsilon$. The transformation matrix [T_4] links these two vectors, with the following expression:

$$\begin{Bmatrix}\alpha\\ \beta\end{Bmatrix}_\varepsilon = [T_4]\{\alpha\}_\varepsilon \quad (16)$$

The new strain energy expression after transformation [T_4], is noted U_d^*; by introducing the expression (16) in (13):

$$\begin{aligned} U_d^* &= \frac{1}{2}\{\alpha\}_\varepsilon^T[T_4]^T[D][T_4]\{\alpha\}_\varepsilon \\ &= \frac{1}{2}\{\alpha\}_\varepsilon^T\left[K^*\right]\{\alpha\}_\varepsilon \end{aligned} \quad (17)$$

is obtained.

To show how to calculate the matrix [K^*], the matrix [D] is decomposed in four sub-matrices.

$$\begin{bmatrix}[D_{11}] & [D_{12}]\\ [D_{21}] & [D_{22}]\end{bmatrix}\begin{Bmatrix}\{\alpha\}_\varepsilon\\ \{\beta\}_\varepsilon\end{Bmatrix} = \begin{Bmatrix}\{F\}_\alpha\\ \{F\}_\beta\end{Bmatrix} \quad (18)$$

where $\{F\}_\alpha$, $\{F\}_\beta$ are the force vectors associated respectively with the two vectors $\{\alpha\}_\varepsilon$ and $\{\beta\}_\varepsilon$. The technique of static condensation consists in reducing the size of the system (18) by expressing the vector $\{\beta\}_\varepsilon$ in function of the vector $\{\alpha\}_\varepsilon$.

$$\{\beta\}_\varepsilon = -\,[D_{22}]^{-1}[D_{21}]\{\alpha\}_\varepsilon. \quad (19)$$

and the system (18) is reduced leading to the following form:

$$[D_{11}] - [D_{12}][D_{22}]^{-1}[D_{21}]\{\alpha\}_\varepsilon = \{F\}_\alpha \quad (20)$$

$$[K^*]\{\alpha\}_\varepsilon = \{F\}_\alpha \quad (21)$$

Thus the expression of the matrix K^* is deduced:

$$[K^*] = [D_{11}] - [D_{12}][D_{22}]^{-1}[D_{21}] \quad (22)$$

At the end of these developments, it can be noted that only the components of the vector $\{\alpha\}_\varepsilon$ appear in the expression of the strain energy U_d^* given by (17); they are the same strain components that appear in the

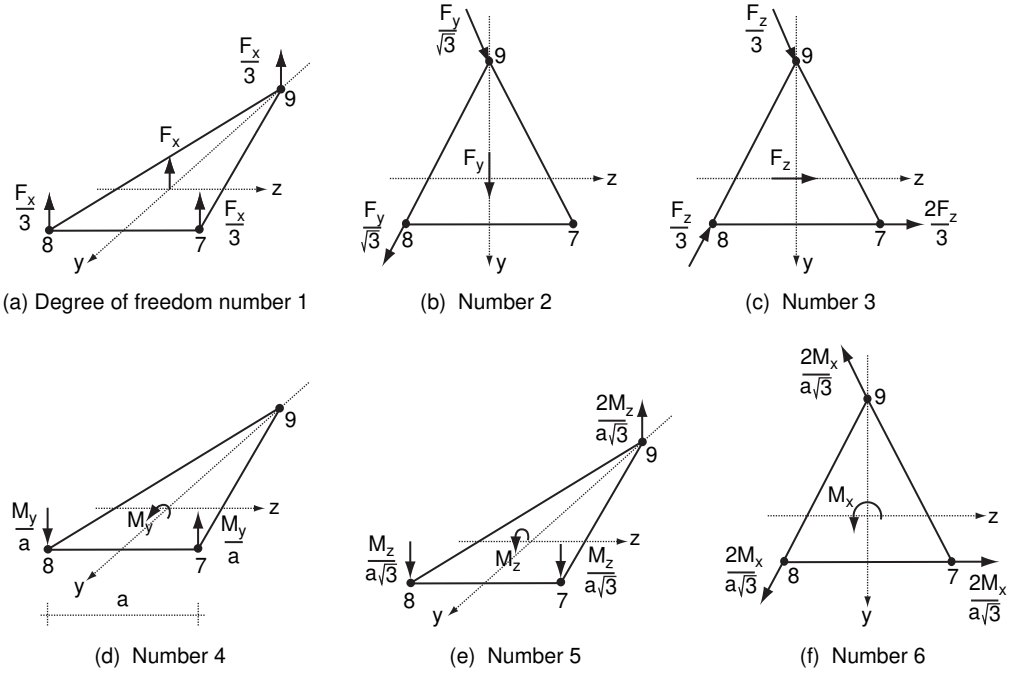

Figure 1. Loadings conditions for the six degrees of freedom.

expression (1). Consequently, a simple analogy between the matrix [K*] and the matrix given by the expression (1) enables the deduction of the equivalent rigidity and the coupling terms of the discrete system.

4. LOADINGS CONDITIONS IN THE FINITE ELEMENT METHODS

Aiming to validate the results by finite element methods in the calculation of the equivalent rigidities, we applied loadings conditions on the cell along the six degrees of freedom. They are displayed for a triangular disposition (such as "simplex" case), in the Figure [1] below:

As an example, in order to calculate the axial stiffness EA and the torsional rigidity GJ (and eventually the coupling term C_{16} between EA and GJ), it is sufficient to apply a unit load $F_x = 1$ along the degree of freedom number 1; the cell will undergo, besides the average axial lengthening d_1, an average rotation d_6. By writing the two equations which include the displacements d_1 and d_6, we obtain:

$$\begin{aligned} \frac{\overline{EA}}{h} d_1 + C_{16} d_6 &= 1 \\ C_{16} d_1 + \frac{\overline{GJ}}{h} d_6 &= 0 \end{aligned} \tag{23}$$

Let us proceed similarly, by applying then a unitary couple $M_x = 1$ along the degree of freedom number 6. The displacements due to a unitary couple are noted d'_1 and d'_6. Therefore we may report the following system:

$$\begin{aligned} \frac{\overline{EA}}{h} d'_1 + C_{16} d'_6 &= 0 \\ C_{16} d'_1 + \frac{\overline{GJ}}{h} d'_6 &= 1 \end{aligned} \tag{24}$$

Working with these two systems, we can calculate the axial stiffness EA and the torsional stiffness GJ and eventually the coupling term C_{16} between the two. We use the same method to calculate the flexural stiffness EI, the shear stiffness GA and the coupling terms between them. For more details, the reader may refer to the reference [16].

5. NUMERICAL APPLICATIONS

Three tensegrity cells are concerned in this study, the simplex, the regular quadruplex *(vertical quadruplex)* and the half-cuboctahedron quadruplex *(horizontal quadruplex)*. Before developing the numerical applications, it is important to remember that the notion of repetitive cell is defined as the assemblies of two cells for the first two cases (Fig 2 and 9). The third case is devoted to only one cell (Fig 15).

For the three cells, the geometrical and mechanical characteristics of the struts and cables are:

Cable cross-section: $A_c = 0.28$ cm^2 ; Strut cross-section: $A_b = 3.25$ cm^2

Young's modulus: $E_c = 40\,000$ Mpa (cables); $E_b = 200\,000$ Mpa (struts)

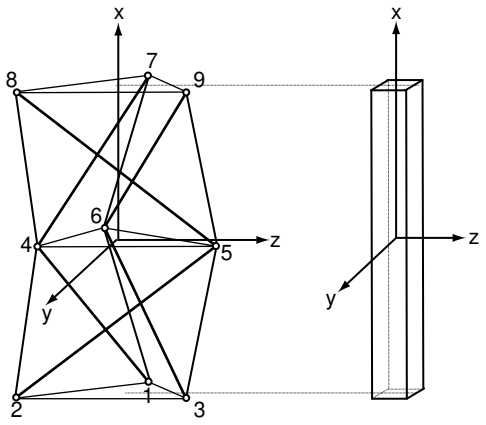

Figure 2. Discrete model and continuum model.

Table 1. Simplex geometry

Nodes	X(cm)	Y(cm)	Z(cm)
1	–95.4	57.7	0
2	–95.4	–28.9	–50
3	–95.4	–28.9	50
4	0	–50	–28.9
5	0	0	57.7
6	0	50	–28.9
7	95.4	57.7	0
8	95.4	–28.9	–50
9	95.4	–28.9	50

Table 2a. Selfstress state of the simplex

Element number	Node 1	Node 2	Selfstress tension value T^{0k} daN	Element number	Node 1	Node 2	Selfstress tension value T^{0k} daN
1 (cable)	1	2	100	12 (strut)	3	6	–254,2
2 (cable)	2	3	100	13 (cable)	5	9	173.2
3 (cable)	1	3	100	14 (cable)	6	7	173.2
4 (cable)	1	6	173.2	15 (cable)	4	8	173.2
5 (cable)	2	4	173.2	16 (cable)	8	9	100
6 (cable)	3	5	173.2	17 (cable)	7	9	100
7 (cable)	4	5	200	18 (cable)	7	8	100
8 (cable)	5	6	200	19 (strut)	5	8	–254,2
9 (cable)	4	6	200	20 (strut)	6	9	–254,2
10 (strut)	1	4	–254,2	21 (strut)	4	7	–254,2
11 (strut)	2	5	–254,2				

Table 2b. Equivalent rigidities of the simplex

Simplex	Energy Method	F.E.M.
EA in daN	9 237	9 262
EI_y=EI_z in daNcm^2	332 240 742	346 909 090
GA_y=GA_z in daN	26.719	29 873
GJ in daNcm^2	2 862 296	2 895 473

5.1. The simplex

In order to validate the suggested approach, the results obtained are, first of all, compared to those obtained with the finite element method (Table 2b), and those for the following initial selfstress tension vector (T°):

Examining this table, the coupling terms can be noted to be null and the equivalent rigidity of flexion (EI_y=EI_z) and of shearing (GA_y=GA_z) are identical according to y and z. This is justified by the fact that the simplex has symmetry in the y-z plane. The equivalent axial rigidity EA and the torsional rigidity GJ are nearly exact: with an approximation of 99.7% for EA and 98.8% for GJ. For the equivalent deflection rigidity EI and the equivalent shearing rigidity GA, the values obtained are respectively 95.7% and 89.4% of the “exact value”.

Now let us observe, on the following four Figures, the influence of the initial selfstress on the equivalent rigidities of the simplex. The initial rigidity is characterised by the selfstress coefficient δ which is varying from 0 to 15.

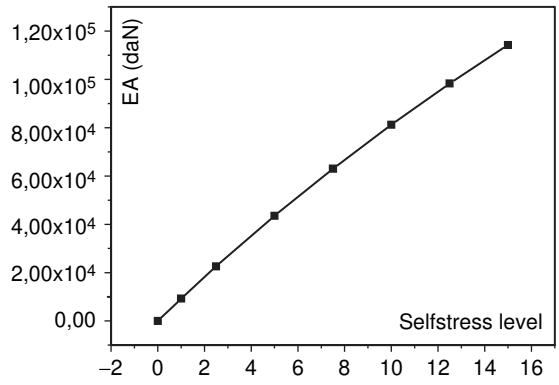

Figure 3. Equivalent axial rigidity EA.

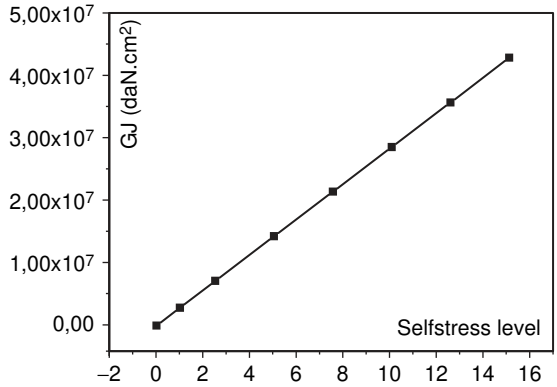

Figure 4. Equivalent torsional rigidity GJ.

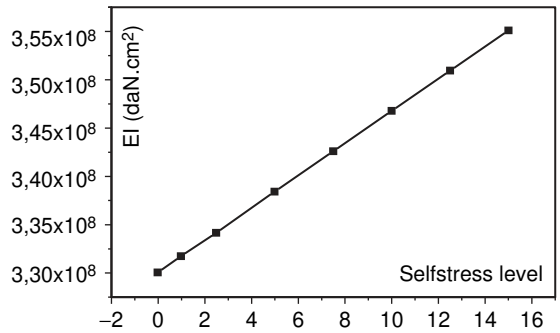

Figure 5. Equivalent rigidity EI.

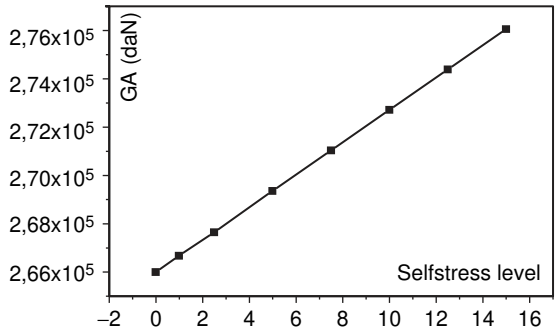

Figure 6. Equivalent shearing rigidity GA.

$q^{(k)} = \delta * \frac{T^{0(k)}}{L^{(k)}}$ *for* $k = 1, b$ Where b is the number of elements

Figure 3 shows that the evolution of the axial rigidity EA in function of the selfstress is almost non-linear, but that in the other three figures (Fig. 4, 5 and 6), the evolution of GJ, EI and of GA with respect to the evolution of the initial selfstress is linear. Moreover, these four figures show a very important result, it concerns the values of certain equivalent rigidities at zero selfstress (in its reference configuration). Figures 3 and 4 do in fact show that axial rigidity EA and torsional rigidity GJ at zero selfstress are null (initial point of the two curves). In other words, the "simplex" in its reference configuration has neither axial rigidity nor torsional rigidity. This result can be explained by the fact that the structure has one infinitesimal mechanism following, which associates a vertical displacement and a rotation around a vertical axis.

To explain the non-linear relationships obtained in Figure [3] between *axial rigidity EA* and the selfstress coefficient δ, we have to underline that the transformation [T4] depends on selfstress. In order to confirm this non linear behaviour, we proposed to compare the results obtained with the finite element method when studying the influence of selfstress on *EA axial rigidity* of simplex. The following figure [7] shows the nonlinear behaviour obtained with the two methods, in spite of the fact that non linearity is little less apparent in the finite element method. It is useful to recall that the equivalent axial rigidity is obtained by a load value equal to 10^3 daN shared between the three high nodes of a simplex module.

To evaluate quantitatively the contribution of the initial selfstress to the equivalent rigidities, the evolution of the adimensional equivalent rigidities (which is the ratio between the equivalent rigidity computed for a given δ and the equivalent rigidity corresponding to δ = 1) in function of the evolution of the selfstress coefficient, is traced (Fig. 8). On this figure, the non-linear evolution of the axial rigidity EA is confirmed. Then, the importance of the contribution of the initial selfstress to the axial rigidity EA and to the torsional rigidity GJ, can be measured. For a selfstress coefficient varying from 1 to 15, the value of EA increases from 9 237.8 daN to 114 209 daN, that is a ratio over 12. As for the value of GJ, it varies between 2 862 296 daNcm^2 and 42 934 170 daNcm^2,

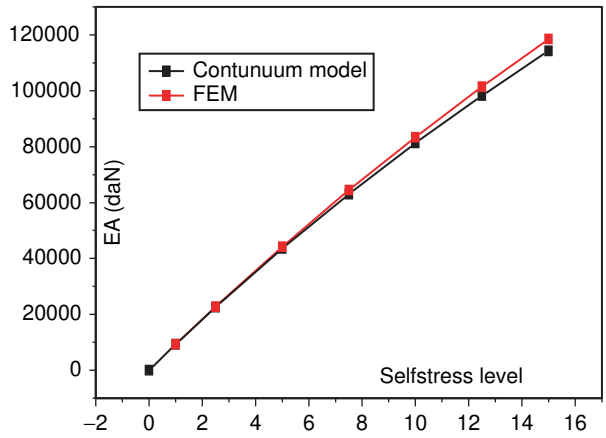

Figure 7. Comparison of results for the equivalent axial rigidity EA.

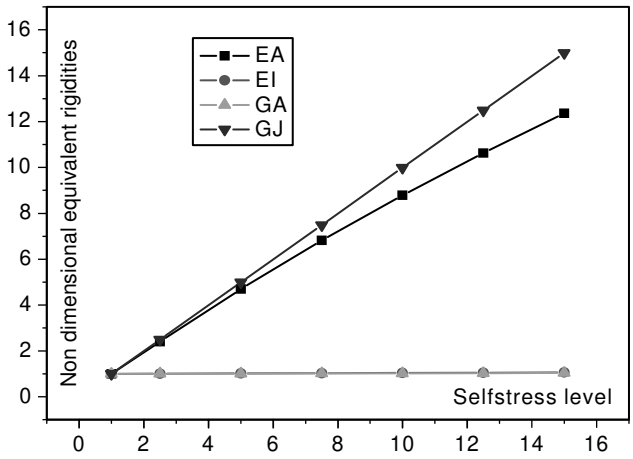

Figure 8. Adimensional equivalent rigidities of the simplex.

Table 3. Quadruplex geometry

Nodes	x(cm)	y(cm)	z(cm)
1	–100	–50	–50
2	–100	50	–50
3	–100	–50	50
4	–100	50	50
5	0	0	–50
6	0	–50	0
7	0	50	0
8	0	0	50
9	100	–50	–50
10	100	50	–50
11	100	–50	50
12	100	50	50

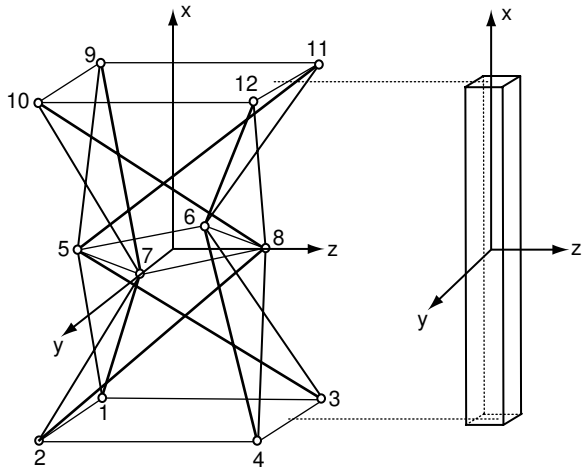

Figure 9. Discrete model and Continuum model.

which corresponds to a ratio of near 15. In contrast to this couple, the evolution of the deflection rigidity EI and of shearing rigidity GA are almost horizontal. For the same evolution of the selfstress coefficient, the value of EI increases from 332 240 742 daNcm^2 to 353 466 964 daNcm^2 which corresponds to a ratio of 1.063 and the value of GA increases from 26 719 daN to 27 620 daN with a ratio of 1.033.

5.2. The vertical quadruplex

Here again, the results are compared to those obtained by the finite element method (Table 4), and those for a vector of initial selfstress tension (T°) daN, such as: (T°)=(100, 100, 100, 100, 282.84, 282.84, 282.84, 282.84, 223.6, 223.6, 223.6, 223.6, –300, –300, –300, –300, 100, 100, 100, 100, 223.6, 223.6, 223.6, 223.6, –300, –300, –300, –300).

The obtained results on the quadruplex are clearly similar to those of the previous application, so the general conclusions are practically the same as for the simplex. The axial equivalent rigidity EA and torsional GJ, are given with a more precise result than the simplex (99.7% for the EA and 99.9% for the GJ). For the equivalent deflection rigidity EI and the equivalent shearing rigidity GA, the obtained values are respectively 89.3% and 92.3% of the “exact value”.

We then tried to evaluate the influence of the initial selfstress on the equivalent rigidities of the quadruplex, keeping the same variation of the selfstress coefficient. Here too, figure 10 shows that the evolution of the axial rigidity EA in function of the selfstress is almost non-linear. In the other three figures, by contrast, (Fig.11, 12 and 13), the evolution of GJ, EI and of GA in function of the evolution of the initial selfstress are linear. These figures also show that the quadruplex (Fig. 9), in its reference configuration, i.e. at zero selfstress, has neither axial rigidity nor torsional rigidity. This result can also be explained, in the same way, by the fact that

Table 4. Equivalent rigidities of the vertical quadruplex

Quadruplex	Energy method	F.E.M.
EA	6339	6355
EI_y=EI_z	319 916 942	285 714 285
GA_y=GA_z	26.188	24 183
GJ	4 000 023	4 000 000

Figure 10. Equivalent axial rigidity EA.

Figure 11. Equivalent torsional rigidity GJ.

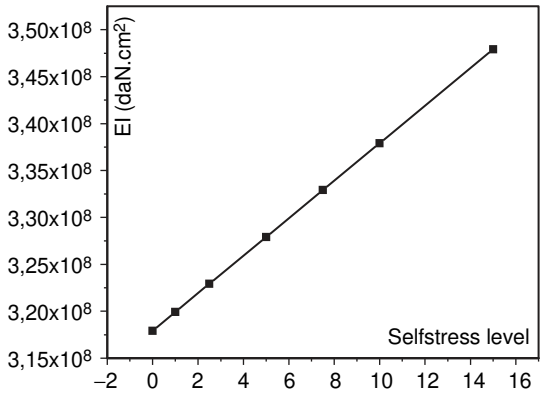

Figure 12. Equivalent deflection rigidity EI.

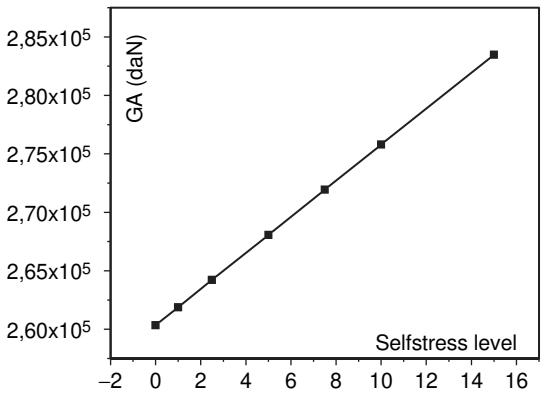

Figure 13. Equivalent shearing rigidity GA.

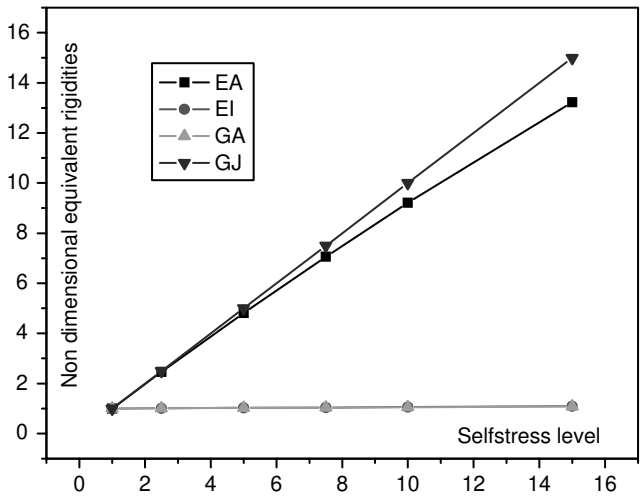

Figure 14. Adimensional equivalent rigidities of the quadruplex.

the structure has one or several infinitesimal mechanisms following these two directions.

The quantitative contribution of the initial selfstress to the equivalent rigidity is easier to see in figure 14, where the evolution of the adimensional equivalent rigidity of the quadruplex in function of the evolution of the coefficient of selfstress is shown. There again, the considerable contribution of the selfstress to the axial rigidity EA and to the torsion rigidity GJ can be measured, and an almost horizontal evolution for the rigidity of flexion EI and of shearing GA. To be more specific, the value of EA increases from 6339 daN to 83 890 daN, which means a ratio of more than 13. The value of GJ increases from 4 000 023 daNcm^2 to 59 997 946 daNcm^2, a ratio of nearly 15. At this point, the selfstress coefficient is also equal to 15, that is to

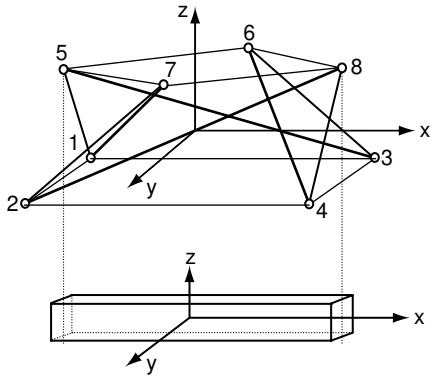

Figure 15. Discrete model and Continuum model.

Table 5. Quadruplex geometry

Nodes	x	y	z
1	–50	–50	–25
2	–50	50	–25
3	50	–50	–25
4	50	50	–25
5	–50	0	25
6	0	–50	25
7	0	50	25
8	50	0	25

say that the slope of evolution of the torsional rigidity GJ is exactly equal to 45°. The value of EI increases from 319 916 942 daNcm^2 to 347 914 516 daNcm^2 corresponding to a ratio of 1.087 and the value of GA increases from 26 188 daN to 28 347 daN with a ratio of 1.082. This means that the equivalent rigidity following these two loads is, for a large part, that of the elastic rigidity of the elements.

5.3. The horizontal quadruplex, an atypical case

The quadruplex homogenized horizontally is an atypical case; the structure can be seen on figure 15 to have no symmetry with respect to the plane perpendicular to the axis of homogenization (yz plane). This why the equivalent deflection rigidity and of shearing rigidity following the two axes y and z are different, and moreover, several coupling terms appear between the different loads. In a previous study on the mechanical behaviour of this same cell, Kebiche et al. (15) showed that under axial load for example, the section represented by the nodes 3, 4 and 8 undergoes several types of strain, and since only the final state of the section is known, the part played by the displacements in each strain cannot be deduced. But it is difficult to find the equivalent rigidities and the coupling terms with the finite element method. Whereas the approach suggested in this study gives us these parameters whatever the complexity of the geometry of the structure.

The results obtained on this module for several values of initial selfstress (the coefficient of selfstress varies from 0 to 10) are presented in the following figures; we have observed the equivalent rigidity and certain coupling terms, the most important being: P_{16}, P_{36}, P_{46}, P_{13}, P_{14} and P_{34}.

The first three figures represent the equivalent rigidity, where we have grouped those cases (Fig.18) of the same size order. The figures 16 and 17 show respectively the evolution of the axial rigidity EA and the shear rigidity GA_y following the axis y in function of the selfstress. For these two rigidities, the evolution is highly non-linear, at the end of this non-linearity ($q_0 = 10$) the curve tends to become horizontal, which means that beyond a certain value of the selfstress, the evolution of this equivalent rigidity is stationary. In figure 16 the evolution of GJ, EI_y and EI_z can be seen to be linear, the influence of the selfstress on the torsion rigidity GJ is greater than the other two. The flexion rigidity EI_y is « two and a half times » greater than the deflection rigidity EI_z ; but the contribution of the selfstress is the same to both rigidities since the two curves are parallel. Finally it is to be noted that the shear rigidity GA_z following z is practically nil.

As for the coupling terms, in figure 19 the most important contribution to the selfstress is recorded on term P_{36}. This term translates the coupling between torsion and deflection along z direction; on the other two terms P_{16} and P_{46}, the influence of the selfstress is much less important, and the evolution is practically horizontal. Figure 20 shows a non-linear evolution of certain coupling terms, the term P_{34} that translates the coupling between the deflection following a transversal axis and the shearing following the other axis, presents a digressive non-linear evolution. The more the selfstress increases, the more the coupling decreases, until a certain value, where it becomes independent of the selfstress. The term P_{13} which translates the coupling between the axial load and the deflection following z presents a progressive non-linear evolution until a certain value, the tangent becomes horizontal and the evolution becomes independent of the selfstress. The term P_{14} also presents a non-linear evolution, this non-linearity is less apparent on the figure, only for a problem of scale.

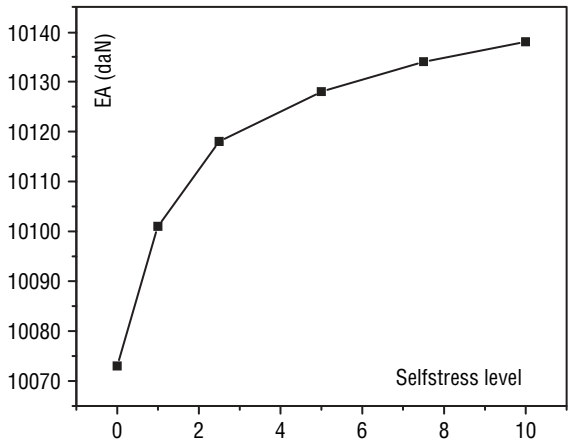

Figure 16. Equivalent deflection rigidity EA.

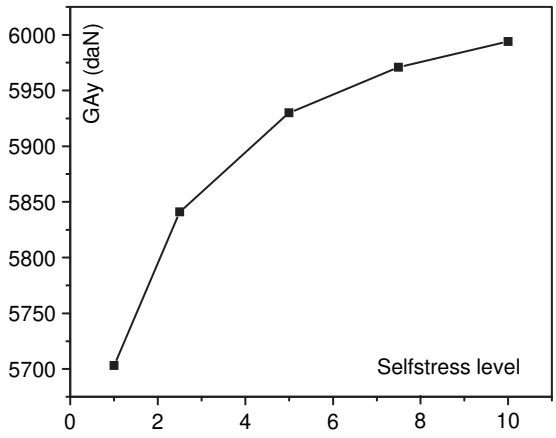

Figure 17. Equivalent shearing rigidity GAy.

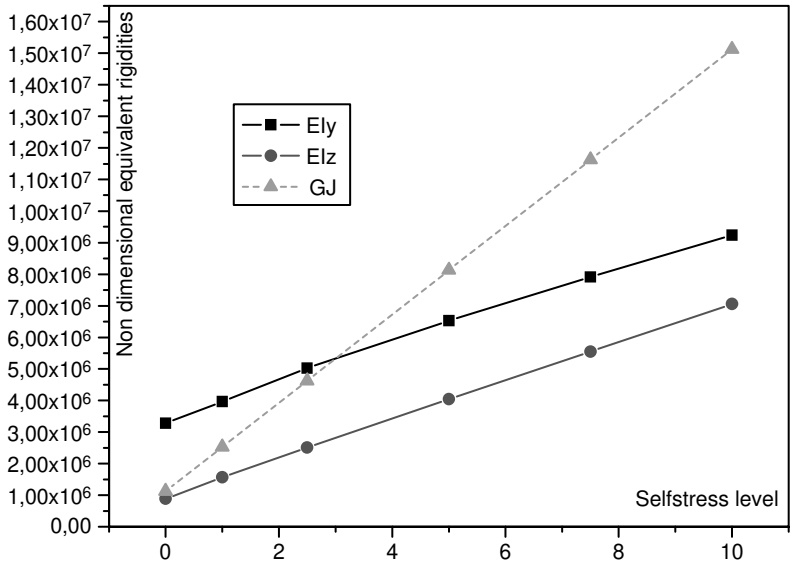

Figure. 18. Equivalent rigidities of the horizontal quadruplex.

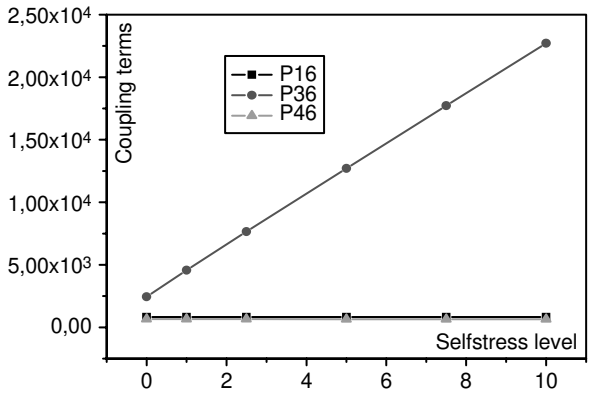

Figure 19. Coupling terms.

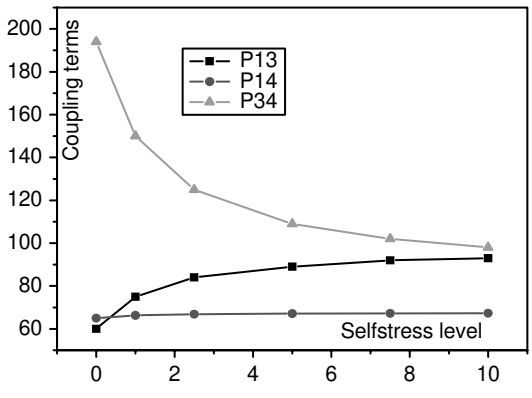

Figure 20. Coupling terms.

Finally, and in order to define the amount of the contribution of the selfstress to the horizontally homogenized quadruplex, the last two figures show the evolution of the adimensional equivalent rigidity (Fig.21) and the adimensional coupling terms (Fig.22) in function of the coefficient of selfstress. In this category of results, we are not interested in the form of the evolution, but in the relative contribution of the

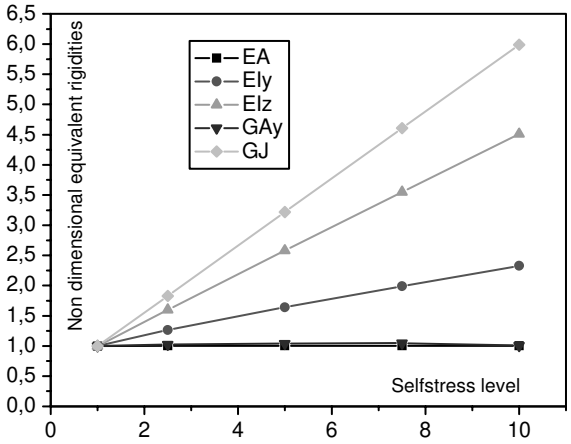

Figure 21. Adimensional equivalent rigidities.

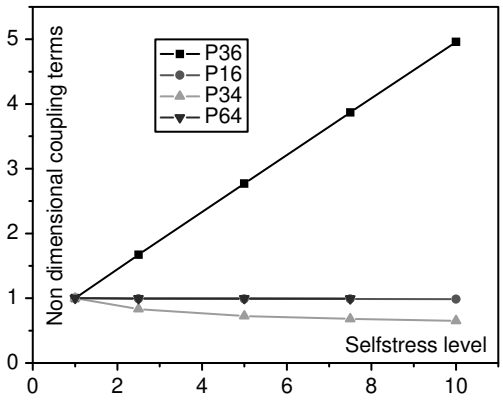

Figure 22. Adimensional coupling terms.

selfstress from one rigidity to another. Thus, it can be noted in figure 19 that the most important contribution is on the torsion rigidity GJ and then the deflection rigidity following z. In this figure the form of the non-linearity of EA and GA_y does not appear just for a problem of scale. In figure 20, the most important contribution of the selfstress is on the coupling term P_{36} followed by the other coupling terms.

6. CONCLUSION

To obtain continuum equivalent properties of systems in selfstress state, an approach based in energy equivalence is suggested. It enables to obtain the parameters that characterize the equivalent continuum model, whatever can be the geometric complexity of the basic cell and the selfstress implemented. In our approach, we have added the transformations necessary on the deformation energy due to the selfstress of the discrete model. Next, a simple analogy with the expression of the total strain energy of the continuum model enables to obtain the equivalent rigidity and the coupling terms of the discrete model. The comparison of the results obtained by this method with those obtained with a direct method (finite element method) gives very satisfactory results.

For each tensegrity module studied, two categories of results have been presented. The first concerns the form of the evolution of the equivalent rigidities and their coupling in function of the selfstress: some behaviours were noted to be linear and others not, namely in the case of the horizontal quadruplex. In the second category of results, we presented the evolution of the adimensional equivalent rigidities and their coupling in function of the selfstress. In this category, we showed that the contribution of the selfstress to certain parameters is very important, and to others almost null.

REFERENCES

[1] Verna P. "*Modélisation continue des structures discrètes par Homogénéisation: cas des treillis*" Thèse de doctorat, Institut National Polytechnique de Grenoble, 1991.

[2] Verna P., Caillerie D. "*Homogénéisation d'un treillis plan hyperstatique intérieurement*" Congrès StruCoMe, Paris, 1990.

[3] Tollenaere H. "*Modèles bidimensionnels de tissés. Homogénéisation des treillis en vibrations libres*" Thèse de doctorat, Institut National Polytechnique de Grenoble, 1994.

[4] Ohayon R. "*Homogénéisation par développements asymptotiques mixtes. Vibrations d'un anneau hétérogène à structure périodique*" CRAS, Paris, t 288, 15 01 1979, Série A.

[5] Noor A.K., Anderson M.C. "*Analysis of Beam-like Lattice Trusses*" Computer Methods in Applied Mechanics and Engineering, Vol.20, 1979, pp. 53–70.

[6] Noor A.K., Anderson M.S., Green W.H. "*Continuum Models for Beam-and Plate-like Lattice Structures*" AIAA Journal, Vol.16, Dec. 1978, pp. 1219–1228.

[7] Noor A.K., Nemeth M.P. "*Analysis of Spatial Beamlike Lattices with Rigid Joints*" Computer Methods in Applied Mechanics and Engineering, Vol.24, 1980, pp. 35–59.

[8] Dow J.O., Su Z., W. Feng C.C. "*Equivalent Continuum Representation of Structures Composed of Repeated Element*s" AIAA Journal, Vol. 23, N.10, Oct 1985, pp. 1564–1569.

[9] McCallen D.B., Romstad K.M. "*A continuum model for the Nonlinear analysis of Beam-like Lattice structures*" Computers & Structures, Vol. 29, N° 2, 1988, pp. 177–197.

[10] Abrate S., Sun C.T. "*Continuum modelling of damping in large space structures*" Proceeding of the second international conference on recent advances in structural dynamics, Vol. II, Inst. of Sound and Vibrations, Res. University of Southampton, Apr 1984, pp. 877–885.

[11] Banks H.T., Crowley J.M. "*Parameter identification in continuum models*" NASA CR-172132, May 1983.

[12] Juang J.N., Sun C.T. "*System identification of large flexible structures by using simple continuum models*" J.Astronaut Sci 31(1), 1983, pp. 77–98.

[13] Yang T.Y., Lamberson S.E. "*Optimization using lattice plate finite elements for feedback control of space structures*" AIAA, Apr 1985, pp.743–750.

[14] Bazant Z.P. "*Micropolar medium as a model for buckling of grid frameworks"* Developments in mechanics, proc. of the 12th midwestern mechanics conference, University of Notre Dame, Notre Dame, IN, Vol 6, Aug 1971, pp 587–593.

[15] Kebiche K, Kazi Aoual MN, Motro R. "*Geometrical nonlinear analysis of tensegrity system*" Engineering Structures Journal, 21, 1999, pp. 864–876.

[16] Ben Kahla « *Equivalent beam-column analysis of guyed towers* » Computers & Structures Vol. 55 No 4, pp.631–645, 1995.